Electric Dipole Polarizability of ^{48}Ca and Implications for the Neutron Skin

J. Birkhan,[1] M. Miorelli,[2,3] S. Bacca,[2,4] S. Bassauer,[1] C. A. Bertulani,[5] G. Hagen,[6,7] H. Matsubara,[8,9]
P. von Neumann-Cosel,[1,*] T. Papenbrock,[6,7] N. Pietralla,[1] V. Yu. Ponomarev,[1] A. Richter,[1]
A. Schwenk,[1,10,11] and A. Tamii[8]

[1]*Institut für Kernphysik, Technische Universität Darmstadt, 64289 Darmstadt, Germany*
[2]*TRIUMF, 4004 Wesbrook Mall, Vancouver, British Columbia V6T 2A3, Canada*
[3]*Department of Physics and Astronomy, University of British Columbia, Vancouver, British Columbia V6T 1Z4, Canada*
[4]*Department of Physics and Astronomy, University of Manitoba, Winnipeg, Manitoba R3T 2N2, Canada*
[5]*Department of Physics and Astronomy, Texas A&M University-Commerce, Commerce, Texas 75429, USA*
[6]*Physics Division, Oak Ridge National Laboratory, Oak Ridge, Tennessee 37831, USA*
[7]*Department of Physics and Astronomy, University of Tennessee, Knoxville, Tennessee 37996, USA*
[8]*Research Center for Nuclear Physics, Osaka University, Ibaraki, Osaka 567-0047, Japan*
[9]*Tokyo Women's Medical University, 8-1 Kawada-cho, Shinjuku-ku, Tokyo 162-8666, Japan*
[10]*ExtreMe Matter Institute EMMI, GSI Helmholtzzentrum für Schwerionenforschung GmbH, 64291 Darmstadt, Germany*
[11]*Max-Planck-Institut für Kernphysik, Saupfercheckweg 1, 69117 Heidelberg, Germany*

The electric dipole strength distribution in ^{48}Ca between 5 and 25 MeV has been determined at RCNP, Osaka from proton inelastic scattering experiments at forward angles. Combined with photoabsorption data at higher excitation energy, this enables the first extraction of the electric dipole polarizability $\alpha_D(^{48}\text{Ca}) = 2.07(22)$ fm^3. Remarkably, the dipole response of ^{48}Ca is found to be very similar to that of ^{40}Ca, consistent with a small neutron skin in ^{48}Ca. The experimental results are in good agreement with *ab initio* calculations based on chiral effective field theory interactions and with state-of-the-art density-functional calculations, implying a neutron skin in ^{48}Ca of 0.14–0.20 fm.

Introduction.—The equation of state (EOS) of neutron-rich matter governs the properties of neutron-rich nuclei, the structure of neutron stars, and the dynamics of core-collapse supernovae [1,2]. The largest uncertainty of the EOS at nuclear densities for neutron-rich conditions stems from the limited knowledge of the symmetry energy J, which is the difference of the energies of neutron and nuclear matter at saturation density, and the slope of the symmetry energy L, which is related to the pressure of neutron matter.

The symmetry energy also plays an important role in nuclei, where it contributes to the formation of neutron skins in the presence of a neutron excess. Calculations based on energy density functionals (EDFs) pointed out that J and L can be correlated with isovector collective excitations of the nucleus, such as pygmy dipole resonances [3] and giant dipole resonances (GDRs) [4], thus suggesting that the neutron skin thickness, the difference of the neutron and proton root-mean-square radii, could be constrained by studying properties of collective isovector observables at low energy [5]. One such observable is the nuclear electric dipole polarizability α_D, which represents a viable tool to constrain the EOS of neutron matter and the physics of neutron stars [6–11].

While correlations among α_D, the neutron skin, and the symmetry energy parameters have been studied extensively with EDFs [12–16], only recently have *ab initio* calculations based on chiral effective field theory (χEFT) interactions

successfully studied such correlations in medium-mass nuclei [17,18]. By using a set of chiral two- plus three-nucleon interactions [19,20] and exploiting correlations between α_D and the proton and neutron radii, Hagen *et al.* predicted, for the first time, the electric dipole polarizability and a neutron skin thickness of 0.12–0.15 fm for ^{48}Ca from an *ab initio* calculation [17]. Since the electric dipole polarizability can be measured rather precisely, this offers novel insights into the properties of neutron-rich matter from a study of the dipole response of ^{48}Ca. The properties of neutron-rich matter also connect this to the physics of the neutron-rich calcium isotopes, with recent pioneering measurements of the masses and 2^+ excitation energies up to ^{54}Ca [21,22] and of the charge radius up to ^{52}Ca [23].

The neutron skin thickness can be obtained by comparison of the matter radii deduced, e.g., from elastic proton scattering [24,25] or coherent photoproduction of neutral pions [26], with well-known charge radii from elastic electron scattering. It can also be measured directly with antiproton annihilation [27,28]. A direct determination of the neutron radius is possible with parity-violating elastic electron scattering. Such an experiment (PREX) has been perfomed at JLAB for ^{208}Pb, but at present, statistical uncertainties limit the precision [29]. A further measurement is approved, and a similar experiment on ^{48}Ca (CREX) is presently under discussion [30,31]. Here, we focus on the electric dipole polarizability

$$\alpha_D = \frac{8\pi}{9} \int \frac{B(E1, E_X)}{E_X} dE_X = \frac{\hbar c}{2\pi^2} \int \frac{\sigma_\gamma(E_X)}{E_X^2} dE_X, \quad (1)$$

where $B(E1)$ and σ_γ denote the electric dipole ($E1$) strength distribution and the $E1$ photoabsorption cross section, respectively, and E_X is the excitation energy. The evaluation of Eq. (1) requires a measurement of the complete $E1$ strength distribution, which is dominated by the GDR [32].

A promising new method to measure the $E1$ strength distribution from low energies across the GDR is inelastic proton scattering under extreme forward angles, including $0°$ at energies of a few hundred MeV [33,34]. In these kinematics, the cross sections are dominated by relativistic Coulomb excitation, while the nuclear excitation of collective modes, except for the spinflip $M1$ resonance [35], is suppressed. Results for α_D extracted for ^{208}Pb [36] and ^{120}Sn [37] have been shown to provide important constraints [38] on the respective neutron skins of these nuclei and, together with data on the exotic nucleus ^{68}Ni from experiments in inverse kinematics [39], on EDFs [14]. In this Letter, we report a measurement for the electric dipole polarizability of ^{48}Ca, which provides the first opportunity to compare with results from *ab initio* calculations based on χEFT interactions and with state-of-the-art EDF calculations in the same nucleus. The insight gained will also impact on the proposed CREX experiment.

Experiments.—The ^{48}Ca(p, p') reaction has been measured at RCNP, Osaka, with an incident proton energy of 295 MeV. Data were taken with the Grand Raiden spectrometer [40] in the laboratory scattering angle range $0°–5.5°$ for excitation energies 5–25 MeV. A ^{48}Ca foil with an isotopic enrichment of 95.2% and an areal density of 1.87 mg/cm^2 was bombarded with proton beams of 4 to 10 nA. Dispersion matching techniques were applied to achieve an energy resolution of about 25 keV (full width at half maximum). The experimental techniques and the raw data analysis are described in Ref. [33], while details for the present experiment can be found in Ref. [41].

Figure 1(a) shows representative spectra taken at laboratory scattering angles $\Theta_{\mathrm{lab}} = 0.4°$ and $2.4°$. At lower excitation energies, a few discrete transitions are observed, mostly of $E1$ character [41]. The prominent transition at 10.23 MeV has $M1$ character [42]. The cross sections above 10 MeV show a broad resonance structure identified with excitation of the GDR. The decrease of cross sections with an increasing scattering angle is consistent with relativistic Coulomb excitation.

Cross sections due to relativistic Coulomb excitation can be separated from the spinflip $M1$ resonance dominating the nuclear response at small momentum transfers using spin transfer observables [36,37] or a multipole decomposition analysis (MDA) of angular distributions [43,44]. Comparison of the two independent methods shows good agreement. No polarization measurements were performed for ^{48}Ca since about 75% of the spinflip $M1$ strength is
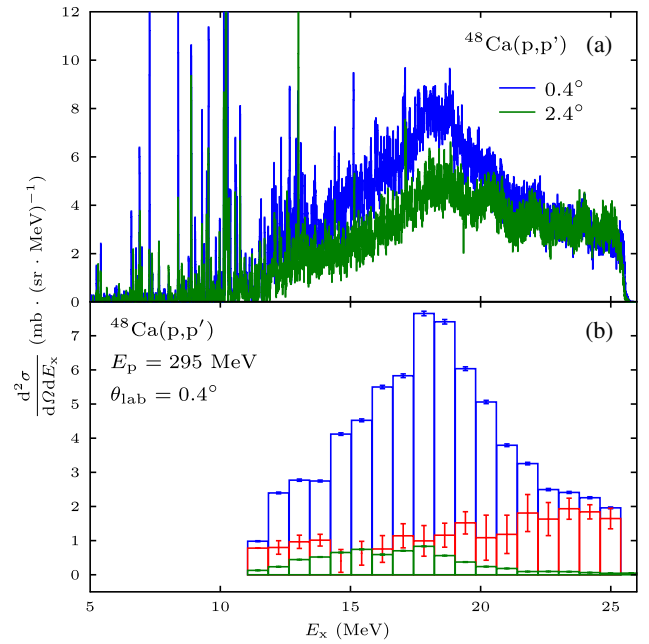

FIG. 1. (a) Spectra of the ^{48}Ca(p, p') reaction at $E_0 = 295$ MeV and scattering angles $\Theta_{\mathrm{lab}} = 0.4°$ (blue) and $2.4°$ (green). (b) Example of the decomposition for the spectrum at $\Theta_{\mathrm{lab}} = 0.4°$. Green histogram: contribution from isoscalar giant resonances subtracted prior to the MDA. Blue histogram: $E1$ part from the MDA. Red histogram: nuclear background from the MDA.

concentrated in the transition at 10.23 MeV, while the rest is strongly fragmented into about 30 weak transitions between 7 and 13 MeV [45].

An angle-independent nuclear background due to quasi-free scattering [46] was included in the MDA. An example of the resulting MDA decomposition is presented in Fig. 1(b). In order to reduce the degrees of freedom in the χ^2 minimization procedure, the cross sections from excitation of the isoscalar giant monopole and quadrupole resonance were determined from the experimental strength functions in ^{48}Ca [47], with the method described in Ref. [44] and subtracted from the spectra. The contributions to the cross sections, shown as the green histogram in Fig. 1(b), are small at the most forward angle (below 10% in any given energy bin).

E1 strength and photoabsorption cross sections.—The Coulomb excitation cross sections resulting from the MDA were converted into equivalent photoabsorption cross sections and a $B(E1)$ strength distribution, respectively, using the virtual photon method [48]. The virtual photon spectrum was calculated in an eikonal approach [49]. The resulting $B(E1)$ strength distribution is displayed as full circles in Fig. 2. The error bars include systematic uncertainties of the absolute cross sections due to charge collection, dead time of the data acquisition, target thickness, as well as a variation of the minimum impact parameter in the calculation of the virtual photon spectrum.
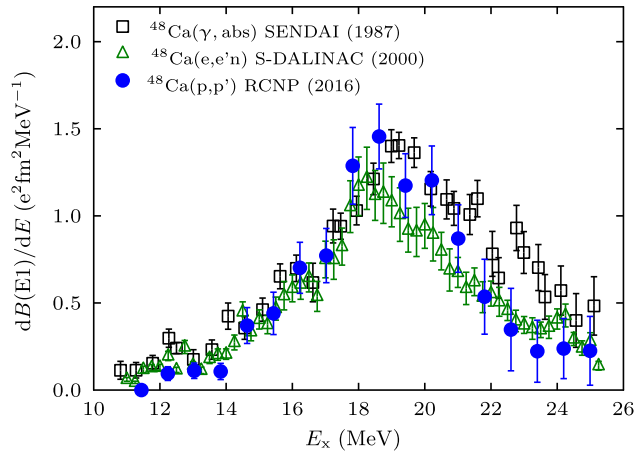
FIG. 2. Comparison of $B(E1)$ strength distributions in ^{48}Ca, deduced from Ref. [50] (squares), Ref. [51] (triangles), and from the present Letter (circles).

The model dependence of the MDA was considered by including the variance of χ^2 values, obtained for fits with all possible combinations of theoretical input curves. The latter contribution dominates the overall uncertainty.

There exist two other measurements of $E1$ strength in ^{48}Ca in the energy region of the GDR. A form factor decomposition of a ^{48}Ca$(e, e'n)$ experiment at the S-DALINAC [51] resulted in the strength distribution shown as open triangles in Fig. 2. Considering that the error bars shown do not include an additional 10% uncertainty from the model dependence of the form factor decomposition [51], the two data sets are in good agreement. However, the proton emission contributes to the cross sections above threshold ($S_p = 15.8$ MeV), although it is expected to be weak in a neutron-rich nucleus. Another result [50] (open squares) shows rather large deviations at the high-energy flank of the GDR. It was obtained from excitation functions of the activity of residual isotopes after particle emission. The photoabsorption cross sections were deduced in an unfolding procedure, with the bremsstrahlung spectrum as an input [52] leading to sizable systematic uncertainties not reflected in the quoted error bars. Furthermore, the contribution from the $(\gamma, 2n)$ channel contributing at higher E_X was estimated from statistical model calculations, assuming a large fraction of direct decay inconsistent with the results of Ref. [51]. Thus, these results are discarded in the following discussion.

From the present Letter, photoabsorption cross sections in the range $E_X = 10$–25 MeV could be extracted and are displayed in Fig. 3(a) as solid dots. They are well described by a Lorentzian, with a centroid energy $E_C = 18.9(2)$ MeV and a width $\Gamma = 3.9(4)$ MeV. The centroid energy is consistent with systematics of the mass dependence [55]

$$E_C = 31.2A^{-1/3} + 20.6A^{-1/6}. \qquad (2)$$

The integrated strength in the measured energy range corresponds to an exhaustion of the $E1$ energy-weighted sum rule of 85%. It is instructive to compare to photoabsorption data
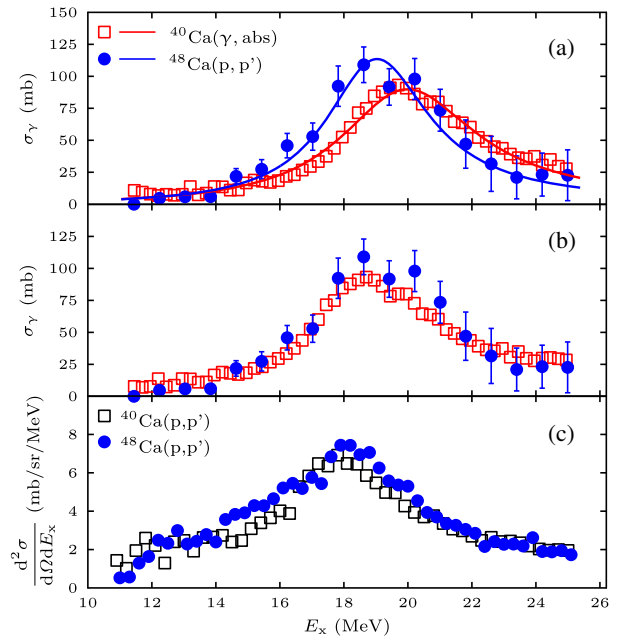

FIG. 3. (a) Photoabsorption cross sections in ^{48}Ca (present Letter, circles) compared with ^{40}Ca (Ref. [53,54], squares). (b) ^{40}Ca data shifted by -0.87 MeV (Eq. (2)). (c) Cross sections of the (p, p') reaction at $E_0 = 295$ MeV and scattering angle $\Theta_{\text{lab}} = 0.4°$ for ^{48}Ca (circles) and ^{40}Ca (squares), the latter shifted by -0.87 MeV.

for ^{40}Ca (open squares) [54], which, again are well described by a Lorentzian. Figure 3(b) compares the two data sets after shifting the ^{40}Ca centroid by the amount predicted by Eq. (2). It is evident that the GDR in ^{40}Ca and ^{48}Ca exhibit nearly identical widths. The contributions to the electric dipole polarizability from the energy region 10–25 MeV are $\alpha_D(^{40}\text{Ca}) = 1.50(2)$ fm^3 and $\alpha_D(^{48}\text{Ca}) = 1.73(18)$ fm^3.

Although the GDR strength dominates, contributions to $\alpha_D(^{48}\text{Ca})$ at lower and higher excitation energies must be considered. Electric dipole strength below the neutron threshold ($S_n = 9.9$ MeV) was measured with the (γ, γ') reaction [56]. Unlike in heavy nuclei, where the low-energy strength is a sizable correction [43,44], the contribution [0.0101(6) fm^3] is negligibly small in ^{48}Ca. For the energy region above 25 MeV, in analogy to the procedure described in Ref. [37], we adopt the ^{40}Ca photoabsorption data of Ref. [53] but shifted by the difference of centroid energies for masses 48 and 40, predicted by Eq. (2). Figure 4(a) summarizes the combined data used for the determination of $\alpha_D(^{48}\text{Ca})$.

The data in Ref. [53] extend up to the pion threshold energy. However, here, we evaluate α_D integrating the strength up to 60 MeV since, as will be shown in the following paragraphs, the sum rule is already well converged at these energies. With these assumptions, we deduce $\alpha_D(^{48}\text{Ca}) = 2.07(22)$ fm^3.

For the comparison with theory, it is instructive to also extract a corresponding value for ^{40}Ca, which one would
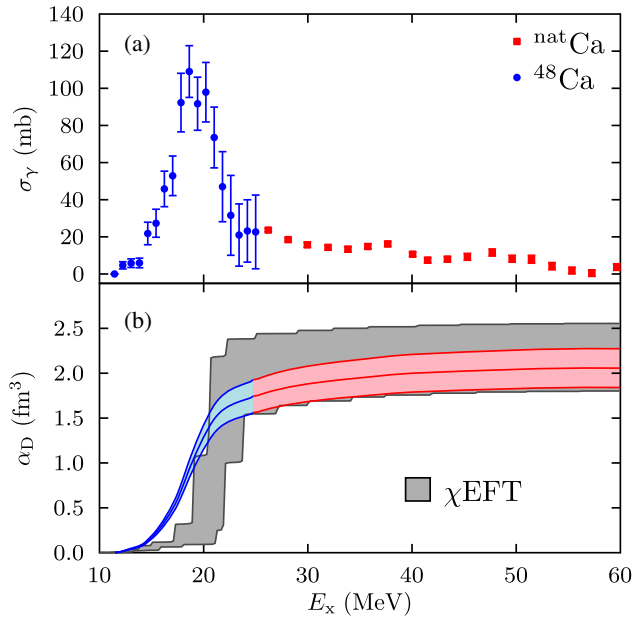
FIG. 4. (a) Combined photoabsorption cross sections in ^{48}Ca from the present Letter (blue circles) for $E_X \leq 25$ MeV and from Ref. [53] (red squares) for $25 \leq E_X \leq 60$ MeV. (b) Running sum of the electric dipole polarizability in comparison to χEFT predictions, where the gray band is based on a set of two- plus three-nucleon interactions [17] and includes a partial uncertainty estimate from the many-body method.

FIG. 5. Experimental electric dipole polarizability in ^{48}Ca (blue band) and predictions from χEFT (green triangles) and EDFs (red squares, for details on the functionals see [17], error bars from Ref. [66]). The green and black bars indicate the χEFT prediction selected to reproduce the ^{48}Ca charge radius [17] and the range of α_D predictions [14] from EDFs providing a consistent description of polarizabilities in ^{68}Ni [39], ^{120}Sn [37], and ^{208}Pb [36], respectively.

expect to be smaller than the one for ^{48}Ca. As shown in Ref. [57], integrating the data for ^{40}Ca from Ref. [53], one obtains $\alpha_D(^{40}$Ca$) = 1.95(26)$ fm^3. Here, we combine the data of Ref. [53] with a refined set of data in the giant resonance region measured by the same group [54] and find $\alpha_D(^{40}$Ca$) = 1.87(3)$ fm^3. We note that a much higher value was quoted in Ref. [53], which would actually exceed our result for ^{48}Ca. The preference of the data set from Ref. [54] is motivated by a preliminary comparison with ^{40}Ca(p, p') results taken at Osaka. Although no $E1$ strength has been extracted yet, a comparison of spectra at the most forward angles [Fig. 3(c)], again shifted by the centroid energy difference, demonstrates good correspondence of the Coulomb excitation cross sections and an absolute ratio similar to the one observed in Fig. 3(b).

Comparison with theory.—First principles calculations of $\sigma_\gamma(E_X)$ require the solution of the many-body scattering problem at all energies E_X, including those in the continuum, which is extremely challenging beyond few-nucleon systems. While an *ab initio* calculation of the full continuum is still out of reach for medium-mass nuclei, methods based on integral transforms that avoid its explicit computation [58–60] have been successfully applied to light nuclei (see Ref. [61] for a review) and recently extended to medium-mass nuclei [57,62,63] using coupled-cluster theory. Furthermore, it has been shown that energy-dependent sum rules, such as the polarizability, can be evaluated without
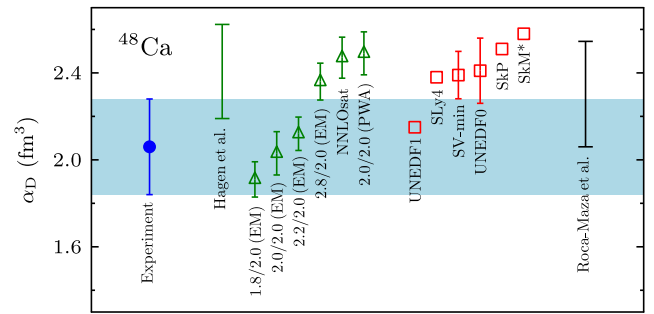
the explicit knowledge of the continuum states or a cross-section calculation itself [64], and recent developments [18] have also allowed the calculation of α_D as a function of the upper integration limit of Eq. (1).

We performed *ab initio* calculations of α_D using the Lorentz integral transform coupled-cluster method described in Refs. [18,57]. The theoretical results are compared to experiment in Fig. 4(b), where the smooth band (blue and red) shows the running sum of the experimental dipole polarizability with error bars. The laddered (gray) band is based on different chiral Hamiltonians, using the same two- and three-nucleon interactions employed in Ref. [17], which reproduce well saturation properties of nuclear matter [19,20,65]. For each interaction, the estimated model-space dependence and truncation uncertainty is about 4% of α_D, which is also included in the gray band. We find that the agreement between the experimental and theoretical results in Fig. 4(b) is better for higher excitation energies. However, we also observed that the position of the GDR is more affected by truncations, which could lead to a shift of ≈ 2 MeV. In addition, we estimated that the contributions from coupled-cluster triples corrections (due to genuine three-particle–three-hole correlations) could be important at low energies. Both of these truncation errors are not included in the uncertainty shown in Fig. 4(b) because it is difficult to quantify them without explicit calculations. With these taken into account, the steep rise in the theoretical band around 20 MeV indicates that the position of the GDR peak is consistent with the experimental centroid.

In Fig. 5, we present a detailed comparison of the experimental α_D value with predictions from χEFT and state-of-the-art EDFs. The χEFT predictions (green triangles) are based on a set of chiral two- plus three-nucleon interactions [19,20], whereas the EDF results are based the functionals SkM*, SkP, SLy4, SV-min, UNEDF0, and UNEDF1 [17]. In addition, we show a χEFT prediction

selected to reproduce the ^{48}Ca charge radius [17] and the range of α_D predictions [14] from EDFs providing a consistent description of polarizabilities in ^{68}Ni [39], ^{120}Sn [37], and ^{208}Pb [36]. Taking only the interactions and functionals in Fig. 5, consistent with the experimental range, implies a neutron skin in ^{48}Ca of 0.14–0.20 fm, where the lower neutron skin in this range (< 0.15 fm) is given by the *ab initio* calculations [17]. For the latter, the small neutron skin is related to the strong $N = 28$ shell closure, which leads to practically the same charge radii for ^{40}Ca and ^{48}Ca.

The *ab initio* results also provide symmetry energy parameter ranges $J = 28.5$–33.3 MeV and $L = 43.8$–48.6 MeV. These constraints are highly competitive, in particular, the value of L, as can be seen in a current comparison of constraints from different methods [67]. The EDF results show larger scattering, in particular, for the density dependence [14].

Summary.—We presented the first determination of the electric dipole polarizability of ^{48}Ca, using relativistic Coulomb excitation in the (p, p') reaction at very forward angles. The resulting dipole response of ^{48}Ca is found to be remarkably similar to that of ^{40}Ca, consistent with a small neutron skin in ^{48}Ca. The result is in good agreement with predictions from χEFT and EDF calculations pointing to a neutron skin of 0.14–0.20 fm.

*vnc@ikp.tu-darmstadt.de

[1] J. M. Lattimer, Annu. Rev. Nucl. Part. Sci. **62**, 485 (2012).
[2] K. Hebeler, J. Holt, J. Menéndez, and A. Schwenk, Annu. Rev. Nucl. Part. Sci. **65**, 457 (2015).
[3] A. Carbone, G. Colò, A. Bracco, L.-G. Cao, P. F. Bortignon, F. Camera, and O. Wieland, Phys. Rev. C **81**, 041301 (2010).
[4] L. Trippa, G. Colò, and E. Vigezzi, Phys. Rev. C **77**, 061304 (2008).
[5] A. Krasznahorkay, M. Fujiwara, P. van Aarle, H. Akimune, I. Daito, H. Fujimura, Y. Fujita, M. N. Harakeh, T. Inomata, J. Jänecke, S. Nakayama, A. Tamii, M. Tanaka, H. Toyokawa, W. Uijen, and M. Yosoi, Phys. Rev. Lett. **82**, 3216 (1999).
[6] B. A. Brown, Phys. Rev. Lett. **85**, 5296 (2000).
[7] R. J. Furnstahl, Nucl. Phys. **A706**, 85 (2002).
[8] M. B. Tsang, J. R. Stone, F. Camera, P. Danielewicz, S. Gandolfi, K. Hebeler, C. J. Horowitz, C. J. Lee, W. G. Lynch, Z. Kohley, R. Lemmon, P. Moller, T. Murakami, S. Riordan, X. Roca-Maza, F. Sammarruca, A. W. Steiner, I. Vidana, and S. J. Yennello, Phys. Rev. C **86**, 015803 (2012).
[9] K. Hebeler, J. M. Lattimer, C. J. Pethick, and A. Schwenk, Astrophys. J. **773**, 11 (2013).
[10] K. Hebeler and A. Schwenk, Eur. Phys. J. A **50**, 11 (2014).
[11] B. A. Brown and A. Schwenk, Phys. Rev. C **89**, 011307 (2014).
[12] P.-G. Reinhard and W. Nazarewicz, Phys. Rev. C **81**, 051303 (2010).
[13] X. Roca-Maza, M. Brenna, G. Colò, M. Centelles, X. Viñas, B. K. Agrawal, N. Paar, D. Vretenar, and J. Piekarewicz, Phys. Rev. C **88**, 024316 (2013).
[14] X. Roca-Maza, X. Viñas, M. Centelles, B. K. Agrawal, G. Colò, N. Paar, J. Piekarewicz, and D. Vretenar, Phys. Rev. C **92**, 064304 (2015).
[15] G. Colò, X. Roca-Maza, and N. Paar, Acta Phys. Pol. B **46**, 395 (2015).
[16] C. Mondal, B. K. Agrawal, M. Centelles, G. Colò, X. Roca-Maza, N. Paar, X. Viñas, S. K. Singh, and S. K. Patra, Phys. Rev. C **93**, 064303 (2016).
[17] G. Hagen, G. Hagen, A. Ekström, C. Forssén, G. R. Jansen, W. Nazarewicz, T. Papenbrock, K. A. Wendt, S. Bacca, N. Barnea, B. Carlsson, C. Drischler, K. Hebeler, M. Hjorth-Jensen, M. Miorelli, G. Orlandini, A. Schwenk, and J. Simonis, Nat. Phys. **12**, 186 (2016).
[18] M. Miorelli, S. Bacca, N. Barnea, G. Hagen, G. R. Jansen, G. Orlandini, and T. Papenbrock, Phys. Rev. C **94**, 034317 (2016).
[19] K. Hebeler, S. K. Bogner, R. J. Furnstahl, A. Nogga, and A. Schwenk, Phys. Rev. C **83**, 031301 (2011).
[20] A. Ekström, G. R. Jansen, K. A. Wendt, G. Hagen, T. Papenbrock, B. D. Carlsson, C. Forssén, M. Hjorth-Jensen, P. Navrátil, and W. Nazarewicz, Phys. Rev. C **91**, 051301 (2015).
[21] F. Wienholtz *et al.*, Nature (London) **498**, 346 (2013).
[22] D. Steppenbeck *et al.*, Nature (London) **502**, 207 (2013).
[23] R. F. Garcia Ruiz *et al.*, Nat. Phys. **12**, 594 (2016).
[24] V. E. Starodubsky and N. M. Hintz, Phys. Rev. C **49**, 2118 (1994).
[25] J. Zenihiro, H. Sakaguchi, T. Murakami, M. Yosoi, Y. Yasuda, S. Terashima, Y. Iwao, H. Takeda, M. Itoh, H. P. Yoshida, and M. Uchida, Phys. Rev. C **82**, 044611 (2010).

[26] C. M. Tarbert *et al.* (Crystal Ball at MAMI and A2 Collaboration), Phys. Rev. Lett. **112**, 242502 (2014).

[27] B. Kłos, A. Trzcinska, J. Jastrzebski, T. Czosnyka, M. Kisielinski, P. Lubinski, P. Napiorkowski, L. Pienkowski, F. J. Hartmann, B. Ketzer, P. Ring, R. Schmidt, T. von Egidy, R. Smolanczuk, S. Wycech, K. Gulda, W. Kurcewicz, E. Widmann, and B. A. Brown, Phys. Rev. C **76**, 014311 (2007).

[28] B. A. Brown, G. Shen, G. C. Hillhouse, J. Meng, and A. Trzcińska, Phys. Rev. C **76**, 034305 (2007).

[29] S. Abrahamyan *et al.* (PREX Collaboration), Phys. Rev. Lett. **108**, 112502 (2012).

[30] J. Mammei, D. McNulty, R. Michaels, K. Paschke, S. Riordan, and P. Souder, Jefferson Lab CREX, 2013.

[31] C. J. Horowitz, K. S. Kumar, and R. Michaels, Eur. Phys. J. A **50**, 48 (2014).

[32] B. L. Berman and S. C. Fultz, Rev. Mod. Phys. **47**, 713 (1975).

[33] A. Tamii *et al.*, Nucl. Instrum. Methods Phys. Res., Sect. A **605**, 326 (2009).

[34] R. Neveling *et al.*, Nucl. Instrum. Methods Phys. Res., Sect. A **654**, 29 (2011).

[35] K. Heyde, P. von Neumann-Cosel, and A. Richter, Rev. Mod. Phys. **82**, 2365 (2010).

[36] A. Tamii *et al.*, Phys. Rev. Lett. **107**, 062502 (2011).

[37] T. Hashimoto *et al.*, Phys. Rev. C **92**, 031305 (2015).

[38] A. Tamii, P. von Neumann-Cosel, and I. Poltoratska, Eur. Phys. J. A **50**, 28 (2014).

[39] D. M. Rossi *et al.*, Phys. Rev. Lett. **111**, 242503 (2013).

[40] M. Fujiwara, H. Akimune, I. Daito, H. Fujimura, Y. Fujita, K. Hatanaka, H. Ikegami, I. Katayama, K. Nagayama, N. Matsuoka, S. Morinobu, T. Noro, M. Yoshimura, H. Sakaguchi, Y. Sakemi, A. Tamii, and M. Yosoi, Nucl. Instrum. Methods Phys. Res., Sect. A **422**, 484 (1999).

[41] J. Birkhan, Doctoral thesis, Technische Universität Darmstadt, 2015.

[42] J. Birkhan, H. Matsubara, P. von Neumann-Cosel, N. Pietralla, V. Y. Ponomarev, A. Richter, A. Tamii, and J. Wambach, Phys. Rev. C **93**, 041302 (2016).

[43] I. Poltoratska *et al.*, Phys. Rev. C **85**, 041304 (2012).

[44] A. M. Krumbholz *et al.*, Phys. Lett. B **744**, 7 (2015).

[45] M. Mathy, J. Birkhan, H. Matsubara, P. von Neumann-Cosel, N. Pietralla, V. Y. Ponomarev, A. Richter, and A. Tamii, Phys. Rev. C **95**, 054316 (2017).

[46] O. Häusser, M. C. Vetterli, R. W. Fergerson, C. Glashausser, R. G. Jeppesen, R. D. Smith, R. Abegg, F. T. Baker, A. Celler, R. L. Helmer, R. Henderson, K. Hicks, M. J. Iqbal, K. P. Jackson, K. W. Jones, J. Lisantti, J. Mildenberger, C. A. Miller, R. S. Sawafta, and S. Yen, Phys. Rev. C **43**, 230 (1991).

[47] Y.-W. Lui, D. H. Youngblood, S. Shlomo, X. Chen, Y. Tokimoto, Krishichayan, M. Anders, and J. Button, Phys. Rev. C **83**, 044327 (2011).

[48] C. A. Bertulani and G. Baur, Phys. Rep. **163**, 299 (1988).

[49] C. Bertulani and A. Nathan, Nucl. Phys. **A554**, 158 (1993).

[50] G. J. O'Keefe, M. N. Thompson, Y. I. Assafiri, R. E. Pywell, and K. Shoda, Nucl. Phys. **A469**, 239 (1987).

[51] S. Strauch, P. von Neumann-Cosel, C. Rangacharyulu, A. Richter, G. Schrieder, K. Schweda, and J. Wambach, Phys. Rev. Lett. **85**, 2913 (2000).

[52] A. S. Penfold and J. E. Leiss, Phys. Rev. **114**, 1332 (1959).

[53] J. Ahrens, H. Borchert, K. Czock, H. Eppler, H. Gimm, H. Gundrum, M. Kröning, P. Riehn, G. S. Ram, A. Zieger, and B. Ziegler, Nucl. Phys. **A251**, 479 (1975).

[54] J. Ahrens, Nucl. Phys. **A446**, 229 (1985).

[55] M. N. Harakeh and A. van der Woude, *Giant Resonances: Fundamental High-Frequency Modes of Nuclear Excitation* (Oxford University, Oxford, 2001).

[56] T. Hartmann, J. Enders, P. Mohr, K. Vogt, S. Volz, and A. Zilges, Phys. Rev. C **65**, 034301 (2002).

[57] S. Bacca, N. Barnea, G. Hagen, M. Miorelli, G. Orlandini, and T. Papenbrock, Phys. Rev. C **90**, 064619 (2014).

[58] V. D. Efros, Sov. J. Nucl. Phys. **41**, 949 (1985).

[59] V. D. Efros, W. Leidemann, and G. Orlandini, Phys. Lett. B **338**, 130 (1994).

[60] V. D. Efros, W. Leidemann, G. Orlandini, and N. Barnea, J. Phys. G **34**, R459 (2007).

[61] S. Bacca and S. Pastore, J. Phys. G **41**, 123002 (2014).

[62] S. Bacca, N. Barnea, G. Hagen, G. Orlandini, and T. Papenbrock, Phys. Rev. Lett. **111**, 122502 (2013).

[63] G. Hagen, T. Papenbrock, M. Hjorth-Jensen, and D. Dean, Rep. Prog. Phys. **77**, 096302 (2014).

[64] N. Nevo Dinur, N. Barnea, C. Ji, and S. Bacca, Phys. Rev. C **89**, 064317 (2014).

[65] C. Drischler, K. Hebeler, and A. Schwenk, Phys. Rev. C **93**, 054314 (2016).

[66] W. Nazarewicz (private communication).

[67] J. M. Lattimer and M. Prakash, Phys. Rep. **621**, 127 (2016).